

## Supporting information

for

### **Performance Enhancement by Additional Donor in D-A-D' Type Thermally Activated Delayed Fluorescence Materials**

Jiuyan Li,<sup>a,b,\*</sup> Xin Li,<sup>c</sup> Jiahui Wang,<sup>b</sup> Jing Jin,<sup>b</sup> Jun Wang<sup>a</sup>

<sup>a</sup> Shandong Laboratory of Advanced Materials and Green Manufacturing at Yantai, Yantai Economic and Technological Development Zone, 300 Changjiang Road, Yantai, 264000, China. E-mail: [greenjiuyanli@amgm.ac.cn](mailto:greenjiuyanli@amgm.ac.cn) (Jiuyan Li).

<sup>b</sup> Frontier Science Center for Smart Materials, College of Chemical Engineering, Dalian University of Technology, 2 Linggong Road, Dalian, 116024, China.

<sup>c</sup> Huawei Device Co., Ltd., Huawei Base, Xiliu Beipo Village, Huanhu Road, High-tech Industrial Development Zone, Songshan Lake, Dongguan, Guangdong Province, China.

## **1. Experimental section**

### **General information**

The  $^1\text{H}$  NMR spectra were measured on a 400 MHz Bruker Avance II 400 using  $\text{CDCl}_3$  as the solvent. Tetramethyl silane (TMS) was used as an internal reference. The  $^{13}\text{C}$  NMR spectra were recorded by AVANCENEO 500 M using Chloroform-d ( $\text{CDCl}_3$ ) as the solvent. The mass spectra were recorded by HP1100LC/MSD MS spectrometer and matrix-assisted laser desorption/ionization (MALDI) micro mass spectrometry (MS) spectrometer. The ultraviolet-visible (UV-Vis) absorption spectra were recorded on a Perkin-Elmer Lambda 750S spectrophotometer. Fluorescence spectra and transient photoluminescence (PL) decay at room temperature were measured with an Edinburgh FLS1000 fluorescence spectrometer. Low temperature phosphorescence spectra were measured on a Hitachi F-7000 fluorescence spectrometer at 77 K in toluene. Cyclic voltammetry (CV) curves were achieved with a CHI610E electrochemical work station, with glass-carbon as the working electrode, a saturated calomel electrode (SCE) as reference electrode and a Pt wire as counter-electrode. Oxidation and reduction curves were obtained in the 0.1 M solutions in dichloromethane (DCM) and dimethylformamide (DMF), respectively with  $n\text{-Bu}_4\text{NPF}_6$  as the supporting electrolyte. Absolute photoluminescence quantum yields (PLQYs) of the compounds were measured in doped and neat films on a HAMAMATSU absolute PL quantum yield spectrometer (C11347).

### **Kinetic parameters calculation of photophysical processes**

The prompt fluorescence lifetimes ( $\tau_{\text{PF}}$ ) were determined by time correlated single photon counting (TCSPC) method with a 375 nm picosecond pulsed LED as the excitation source at room temperature. And delayed fluorescence lifetimes ( $\tau_{\text{DF}}$ ) were measured using multi-channel scaling (MCS) as data acquisition technique with a 365 nm variable pulsed LED as the excitation source and at room temperature. The lifetimes were calculated using the following equations:

$$(S1) \quad \tau = \frac{B_1\tau_1^2 + B_2\tau_2^2 + B_3\tau_3^2}{B_1\tau_1 + B_2\tau_2 + B_3\tau_3}$$

The equations used to calculate the excited state kinetics parameters are as follows.

$$(S2) \quad k_p = 1 / \tau_{\text{PF}}$$

$$(S3) \quad k_d = 1 / \tau_{\text{DF}}$$

$$(S4) \quad k_r = \Phi_{\text{PF}} / \tau_{\text{PF}}$$

$$(S5) \quad \Phi_{\text{PL}} = k_r / (k_r + k_{\text{nr}})$$

$$(S6) \quad \Phi_{\text{PF}} = k_r / (k_r + k_{\text{ISC}} + k_{\text{nr}})$$

$$(S7) \quad k_{\text{RISC}} = k_p k_d \Phi_{\text{DF}} / k_{\text{ISC}} \Phi_{\text{PF}}$$

$k_p$  and  $k_d$  represent the rate constants of prompt process and delay process, while  $k_r$  and  $k_{\text{nr}}$  represent the rate constants of radiation and non-radiation.  $k_{\text{ISC}}$  and  $k_{\text{RISC}}$  represent rate constants of intersystem crossing and reverse intersystem crossing,

respectively.  $\Phi_{\text{PL}}$ ,  $\Phi_{\text{PF}}$  and  $\Phi_{\text{DF}}$  represent total PLQY, quantum yield of the prompt component and quantum yield of the delayed component, respectively.  $\tau_{\text{PF}}$  and  $\tau_{\text{DF}}$  represent average lifetimes of the prompt and delayed components, respectively.

## Theoretical calculations

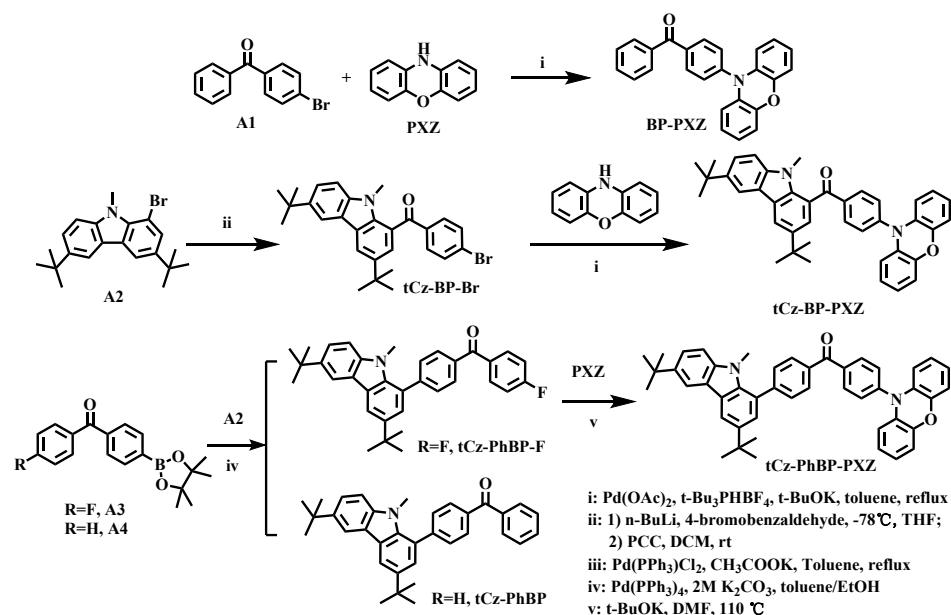
The theoretical calculations were performed with the Gaussian 16 package, using the density functional theory (DFT) and time-dependent density functional theory (TDDFT) method with the B3LYP hybrid functional. The ground states ( $S_0$ ) geometries and the lowest excited singlet and triplet states geometries ( $S_1$  and  $T_1$ ) were optimized through DFT/TD-DFT methods at the B3LYP/6-31g(d) level in the gas phase. The related HOMO and LUMO orbitals, and the natural transition orbitals (NTOs) were analyzed and then plotted through Multiwfn 3.8 and VMD.

## Devices fabrication

The involved functional layer materials except for emitters were gained through commercial sources. The ITO glass substrates with a certain resistance were cleaned in different detergents, and handled in ozone atmosphere for 30 min. For all the devices, the functional layer materials were fabricated with a pressure below  $1 \times 10^{-4}$  Pa. Each device possesses an effective light-emitting area of  $3.0 \times 3.0$  mm<sup>2</sup>. Current density-voltage-luminance ( $J$ - $V$ - $L$ ) curves and electroluminescence (EL) spectra were recorded on Keithley 2400 SMU and a Konica Minolta Chroma Meter CS-200 and HAMAMATSU C9920-11, respectively. All relevant device measurements were operated in the air without further encapsulations. The forward viewing external

quantum efficiency was calculated by using the current efficiency, EL spectra and human photopic sensitivity.

## Compounds syntheses



**Scheme 1** Synthetic Routes of BP-PXZ, tCz-BP-PXZ, tCz-PhBP-PXZ and tCz-PhBP.

**Synthesis of (4-bromophenyl)(3,6-di-tert-butyl-9-methyl-9H-carbazol-1-yl)methanone (tCz-BP-Br).** To a solution of compound A2 (1.86 g, 5 mmol) in 50 mL dried THF that was cooled to -78 °C, n-BuLi (3 mL, 7.5 mmol, 2.5 M) was added dropwise using a syringe under nitrogen. The mixture was stirred for 1 h at -78 °C and then stirred for 2 h at room temperature. Then the mixture solution was cooled to -78 °C again and 4-bromobenzaldehyde (2.7 g, 15 mmol) was slowly added into the reaction solution. The mixture was stirred for 1 h at -78 °C and then stirred overnight at room temperature. Subsequently, the mixture was stirred for 10 minutes under ice-water. Then, 50 mL of ice water was added to quench the reaction and perform a hydrolysis reaction. The resulting mixture was extracted with dichloromethane three

times. The combined organic layers were dried over anhydrous magnesium sulfate. After filtration and solvent evaporation, the crude product was dissolved in 20 mL of dichloromethane in a 100 mL round bottom flask, then pyridinium chlorochromate (PCC, 3.23 g, 15 mmol) was added. The mixture was stirred for 12 h. The precipitate was filtered and the filtrate was evaporated under reduced pressure. After solvent evaporation, the crude product was purified by column chromatography over silica gel with a dichloromethane/petroleum ether mixture as an eluent, providing the product as a yellow solid in 45% yield. <sup>1</sup>H NMR (400 MHz, Chloroform-*d*) δ 8.29 (d, *J* = 1.9 Hz, 1H), 8.13 (d, *J* = 1.8 Hz, 1H), 7.83 – 7.77 (m, 2H), 7.66 – 7.60 (m, 2H), 7.57 (dd, *J* = 8.7, 1.9 Hz, 1H), 7.48 (d, *J* = 1.9 Hz, 1H), 7.32 (d, *J* = 8.7 Hz, 1H), 3.55 (s, 3H), 1.47 (s, 9H), 1.43 (s, 9H).

**Synthesis of ((4-(3,6-di-*tert*-butyl-9-methyl-9H-carbazol-1-yl)phenyl)(4-fluorophenyl)methanone (tCz-PhBP-F) and (4-(3,6-di-*tert*-butyl-9-methyl-9H-carbazol-1-yl)phenyl)(phenyl)methanone (tCz-PhBP).** To a deoxygenated solution of intermediates 1-bromo-3,6-di-*tert*-butyl-9-methyl-9H-carbazole (A2) (5 mmol), (4-fluorophenyl)(4-(4,4,5,5-tetramethyl-1,3,2-dioxaborolan-2-yl)phenyl)methanone (A3) or phenyl(4-(4,4,5,5-tetramethyl-1,3,2-dioxaborolan-2-yl)phenyl)methanone (A4) (6 mmol), toluene (40 mL), ethanol (8 mL), and aqueous potassium carbonate (2 M, 25 mmol) was added tetrakis(triphenylphosphino)palladium(0) (0.25 mmol) under nitrogen atmosphere. The reaction mixture was refluxed overnight. Upon cooled to room temperature and diluted by water (20 mL), the organic layer was separated and the aqueous layer was extracted with dichloromethane (3 × 20 mL). The combined

organic layers were washed with brine (50 mL), dried over anhydrous magnesium sulfate and filtered. After removing the solvent under reduced pressure, the residue was purified by column chromatography over silica using petroleum ether/chloroform as eluent to give pure product.

**tCz-PhBP-F.** White solid. Yield: 85%.  $^1\text{H NMR}$  (400 MHz, Chloroform-*d*)  $\delta$  8.14 (d,  $J = 6.3$  Hz, 2H), 8.06 – 7.87 (m, 4H), 7.66 (d,  $J = 7.9$  Hz, 2H), 7.55 (d,  $J = 8.4$  Hz, 1H), 7.32 (d,  $J = 22.0$  Hz, 2H), 7.22 (t,  $J = 8.4$  Hz, 2H), 3.39 (s, 3H), 1.50 (q,  $J = 6.4$ , 4.6 Hz, 18H). TOF-EI-MS ( $m/z$ ): cal. for  $\text{C}_{34}\text{H}_{34}\text{FNO}$  491.2624; Found: 491.2614  $[\text{M}]^+$ .

**tCz-PhBP.** Green solid.  $^1\text{H NMR}$  (400 MHz, Chloroform-*d*)  $\delta$  8.14 (dd,  $J = 5.3$ , 1.8 Hz, 2H), 8.01 – 7.81 (m, 4H), 7.64 (dd,  $J = 12.7$ , 7.7 Hz, 3H), 7.58 – 7.48 (m, 3H), 7.35 (d,  $J = 1.8$  Hz, 1H), 7.28 (d,  $J = 9.0$  Hz, 1H), 3.39 (s, 3H), 1.49 (s, 9H), 1.48 (s, 9H). TOF-EI-MS ( $m/z$ ): cal. for  $\text{C}_{34}\text{H}_{35}\text{NO}$  473.2719; Found: 473.2718  $[\text{M}]^+$ . Anal. Calcd for  $\text{C}_{34}\text{H}_{35}\text{NO}$ : C, 86.22; H, 7.45; N, 2.96; Found: C, 86.20; H, 7.44; N, 2.97.

## 2. Supplement Figures and Tables

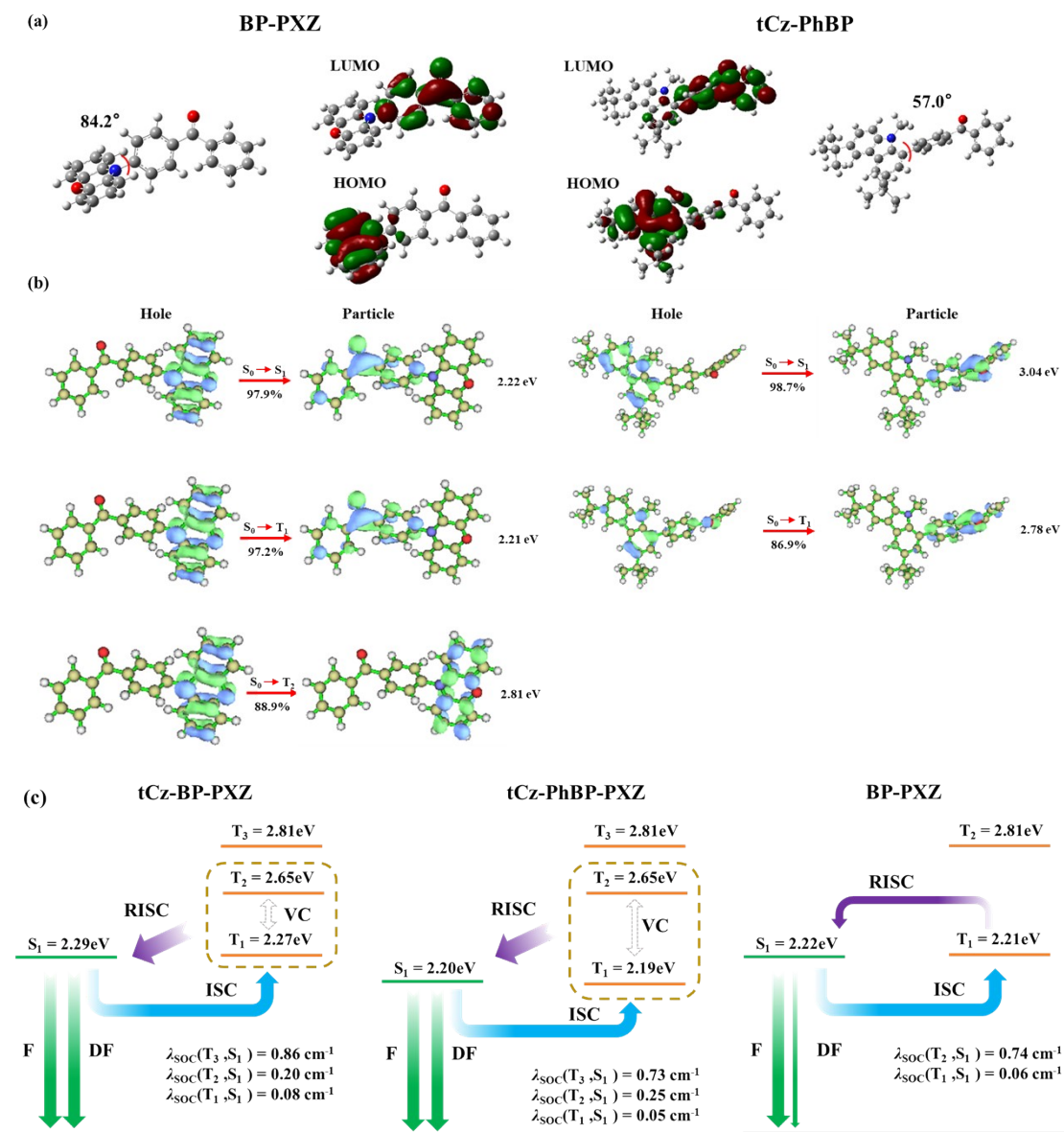


**Fig. S1** Steric geometries and HOMO/LUMO distribution (a) and the NTO analyses of the singlet and triplet excited states (b) for two reference emitters BP-PXZ and tCz-PhBP, and the supposed RISC mechanism for the three TADF emitters in this study (c).

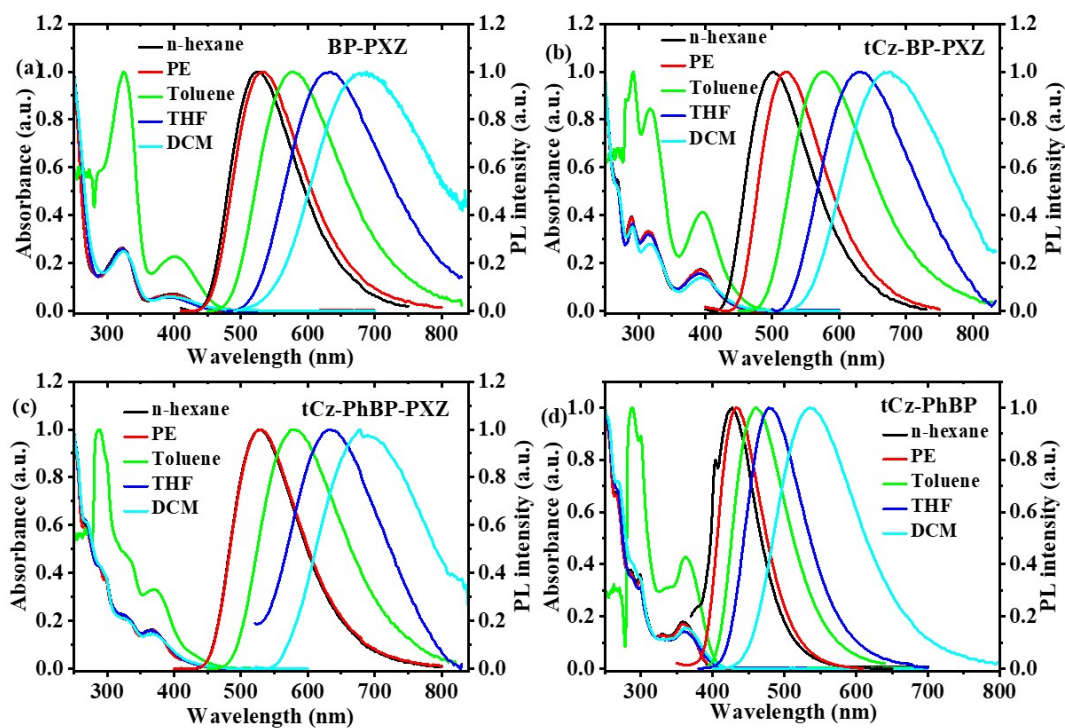


**Fig. S2** PL spectra of the investigated molecules in different solvents.

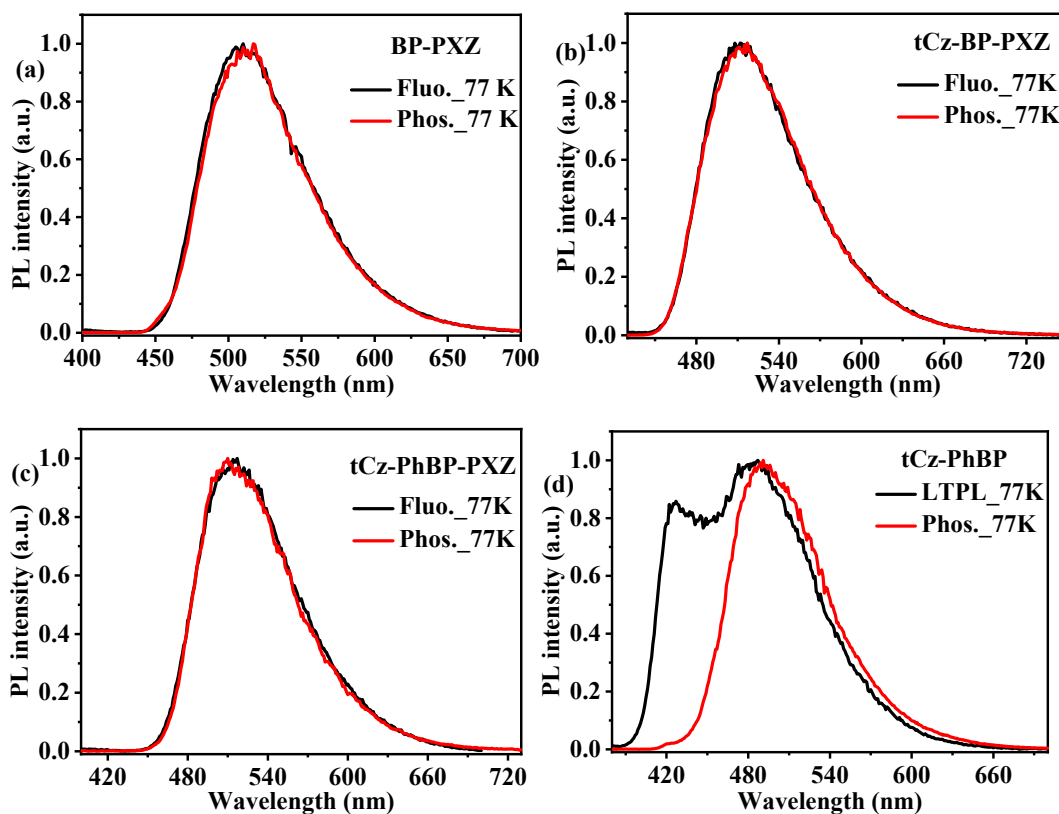


**Fig. S3** The fluorescence and phosphorescence spectra for BP-PXZ, tCz-BP-PXZ, tCz-PhBP-PXZ and tCz-PhBP in frozen toluene at 77 K.

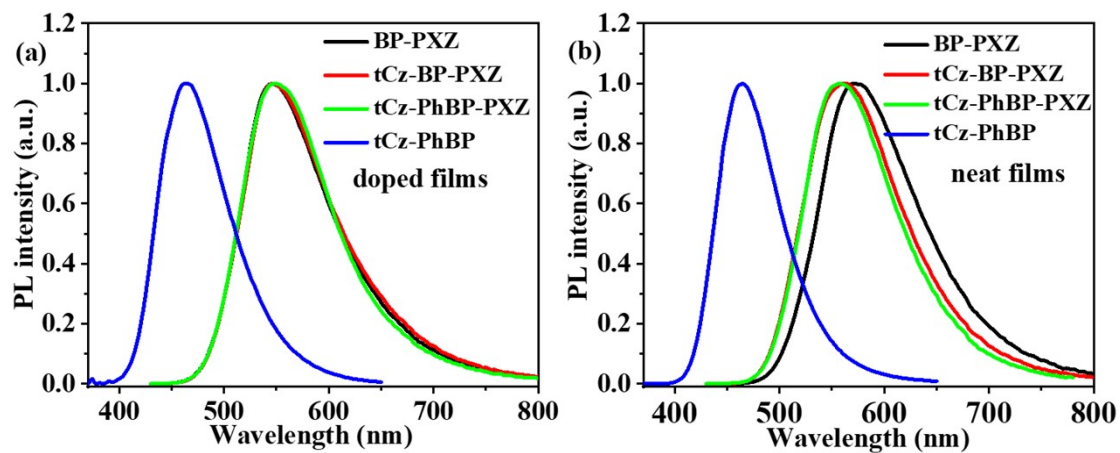


**Fig. S4** PL spectra of BP-PXZ, tCz-BP-PXZ, tCz-PhBP-PXZ and tCz-PhBP in doped films (a, 10%) and in neat films (b).

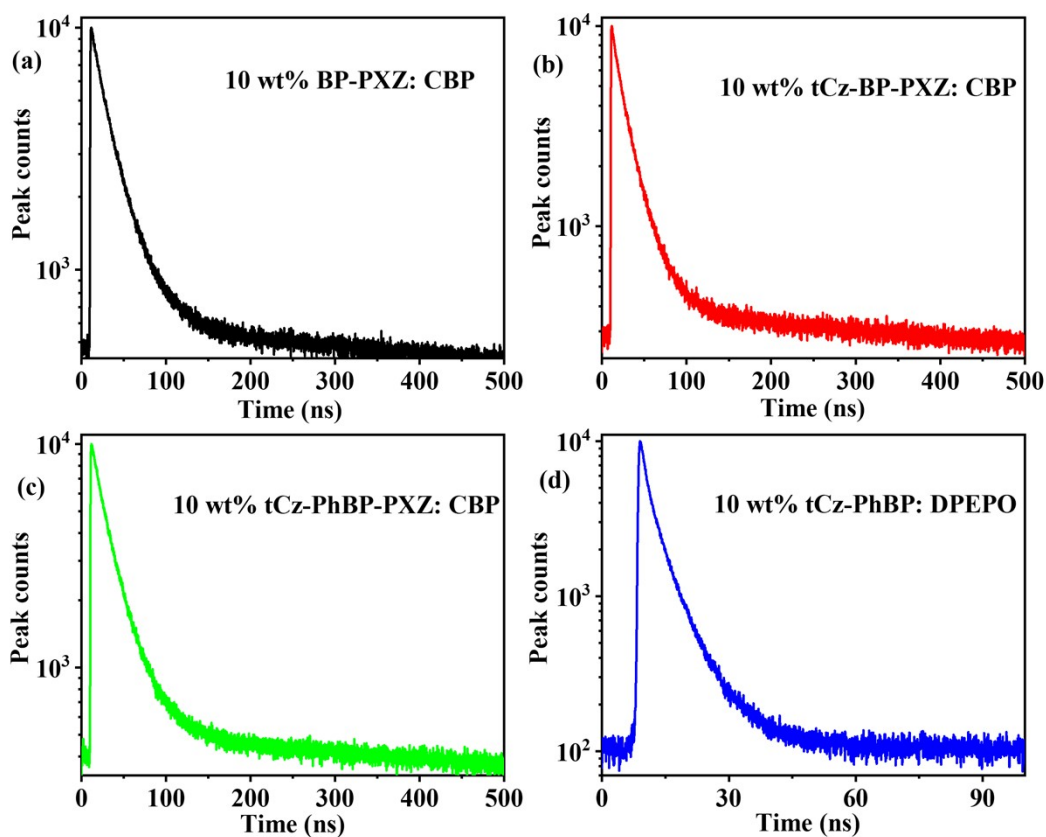


**Fig. S5** Transient PL decay curves of BP-PXZ, tCz-BP-PXZ, tCz-PhBP-PXZ and tCz-

PhBP in doped films measured by TCSPC technique at room temperature.

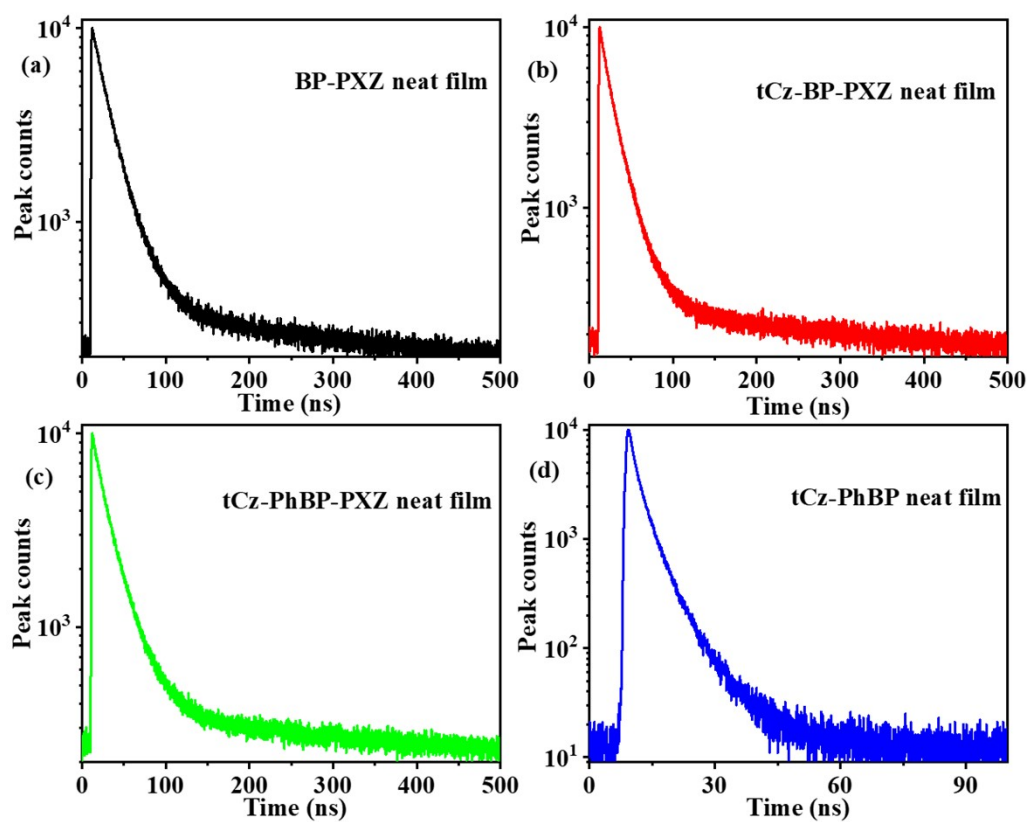


**Fig. S6** Transient PL decay curves of BP-PXZ, tCz-BP-PXZ, tCz-PhBP-PXZ and tCz-PhBP in neat films measured by TCSPC technique at room temperature.

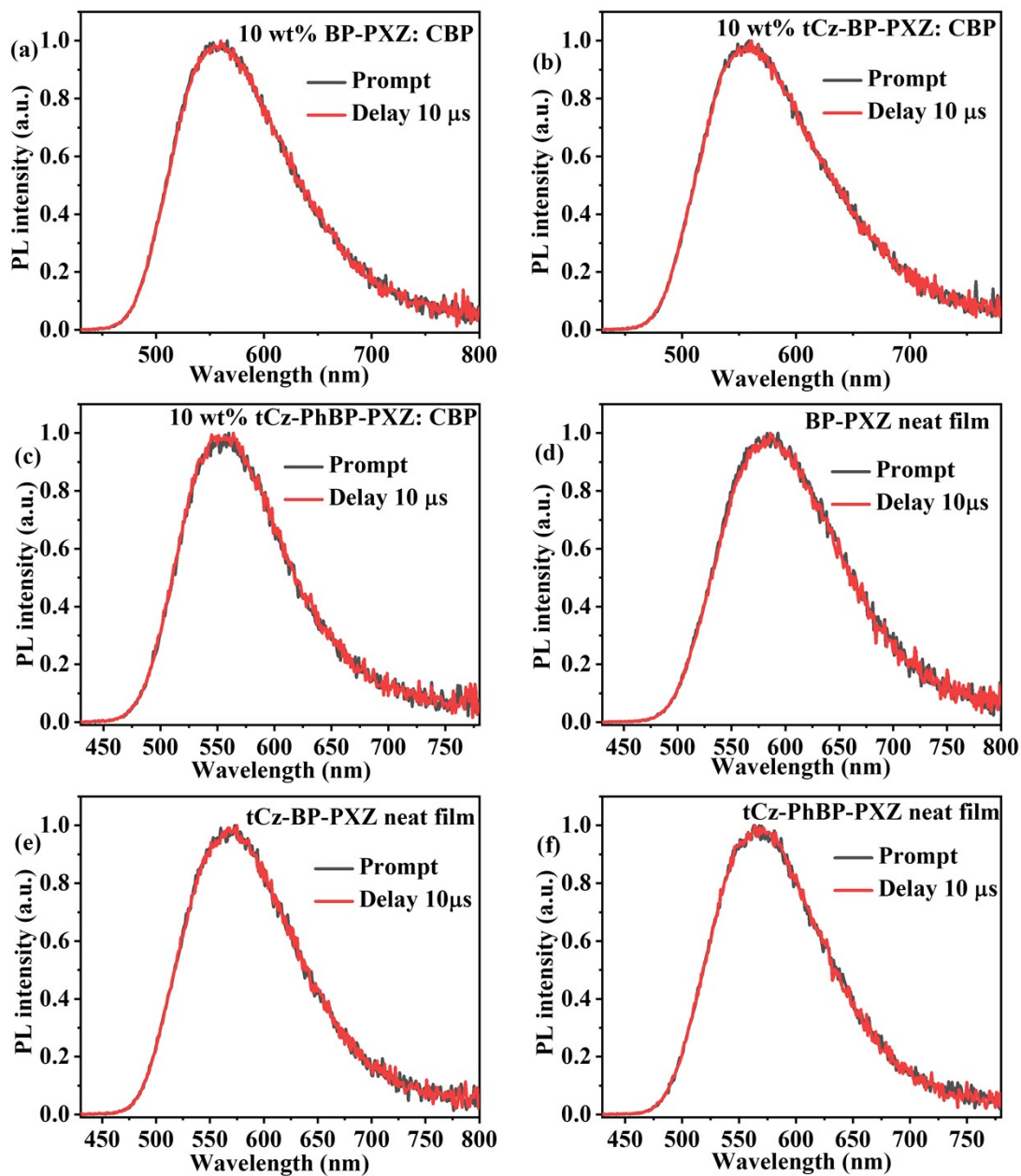


**Fig. S7** The time-resolved spectra of the investigated D-A molecules in the DPEPO doped films (10 wt%).

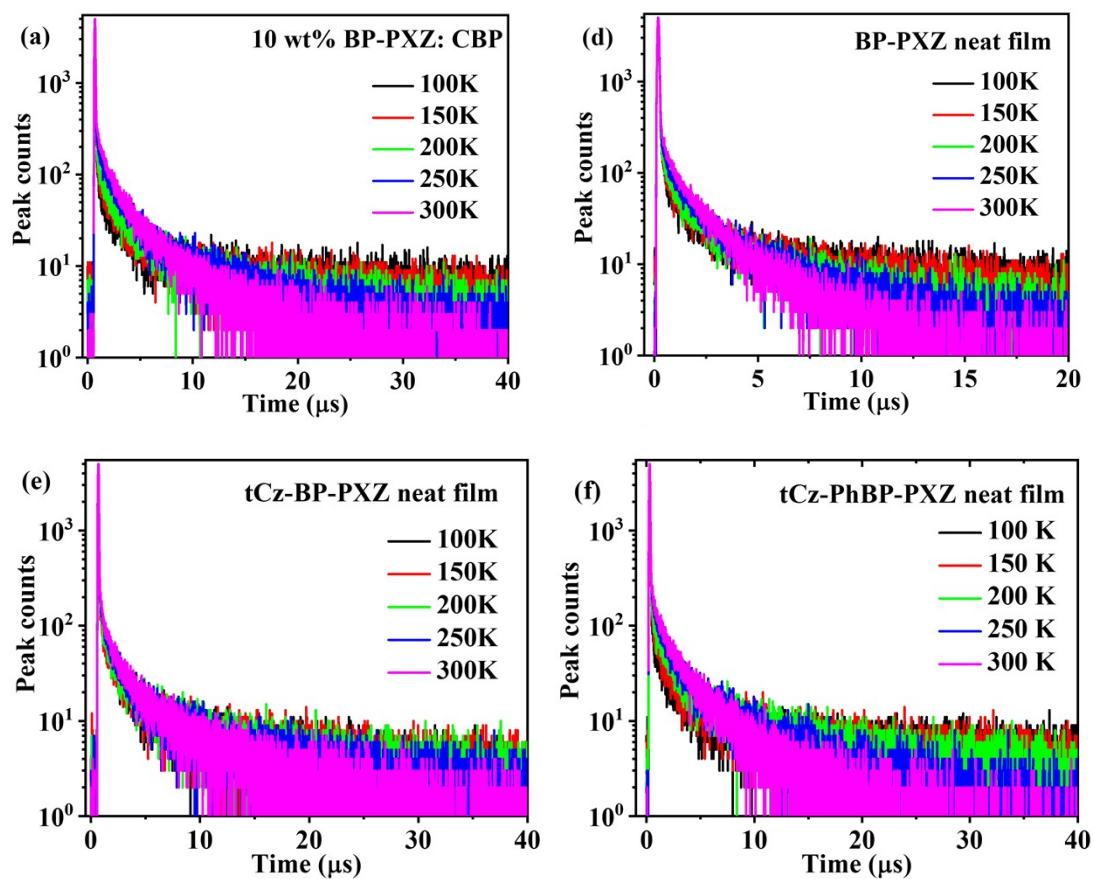


**Fig. S8** Temperature dependent transient PL decay curves of BP-PXZ, tCz-BP-PXZ and tCz-PhBP-PXZ in doped (a) and neat films (d-f) measured at room temperature.

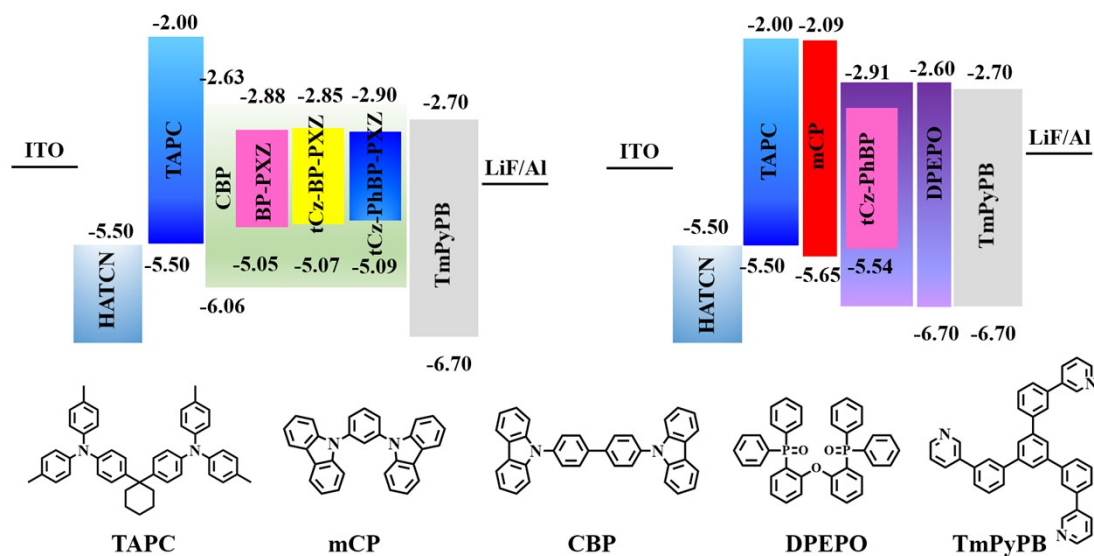


**Fig. S9** The energy diagram for the vacuum deposited OLEDs and chemical structures of the relevant materials used for device fabrication.

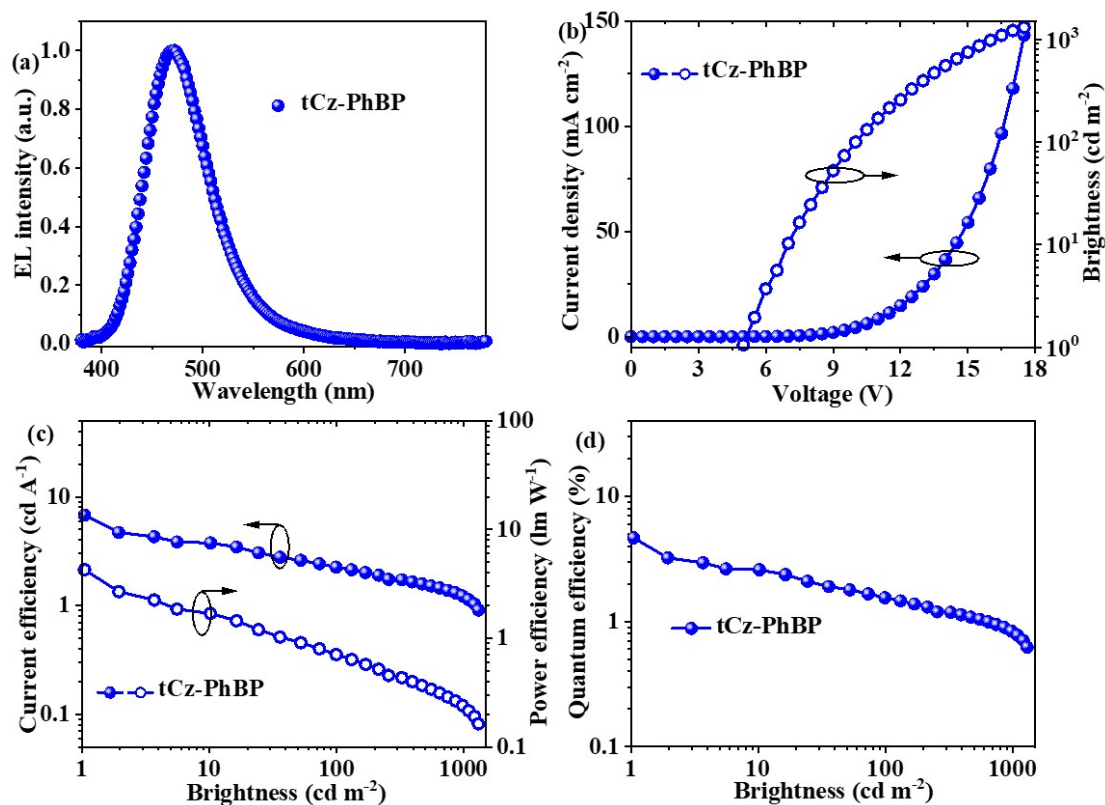


**Fig. S10** EL spectra (a),  $J$ - $V$ - $B$  characteristics (b) and efficiency curves (c and d) for tCz-PhBP based devices A4.

**Table S1** Calculated SOC matrix element values for the TADF emitters.

$\lambda_{\text{SOC}}$ ( $\text{cm}^{-1}$ )/ $\Delta E_{\text{SITn}}$ (eV) /Classification of electronic excitation	BP-PXZ	tCz-BP-PXZ	tCz-PhBP-PXZ
T <sub>1</sub> -S <sub>1</sub>	0.06/0.01/CT(PXZ→BP)	0.08/0.02/CT(PXZ→BP)	0.05/0.02/CT(PXZ→PhBP)
T <sub>2</sub> -S <sub>1</sub>	0.74/-0.59/LE <sub>PXZ</sub>	0.20/-0.36/CT(tCz→BP)	0.25/-0.46/CT(tCz→PhBP)
T <sub>3</sub> -S <sub>1</sub>	0.52/-0.70/	0.86/-0.52/LE <sub>PXZ</sub>	0.73/-0.61/LE <sub>PXZ</sub>

**Table S2** EL Performances of device based on tCz-PhBP.

Device	$V_{\text{on}}$ [V]	$L_{\text{max}}$ [cd m <sup>-2</sup> ]	$\eta_{\text{c}}$ [cd A <sup>-1</sup> ]	$\eta_{\text{p}}$ [lm W <sup>-1</sup> ]	$\eta_{\text{ext}}$ [%]	$\lambda_{\text{EL}}$ [nm]	CIE (x,y)
A4	5.0	1303	6.8	4.3	4.7	472	0.16,0.20

Device structure: ITO/HATCN (10 nm)/TAPC (20 nm)/mCP (10 nm)/DPEPO: 10wt%

tCz-PhBP (30 nm)/TmPyPB (40 nm)/LiF (1 nm)/Al (200 nm).